

Vocal tract modelling in fallow deer: are male groans nasalized?

Article (Accepted Version)

Reby, D, Wyman, M T, Frey, R, Charlton, B D, Dalmont, J P and Gilbert, J (2018) Vocal tract modelling in fallow deer: are male groans nasalized? *Journal of Experimental Biology*, 221 (17). pp. 1-12. ISSN 0022-0949

This version is available from Sussex Research Online: <http://sro.sussex.ac.uk/id/eprint/76812/>

This document is made available in accordance with publisher policies and may differ from the published version or from the version of record. If you wish to cite this item you are advised to consult the publisher's version. Please see the URL above for details on accessing the published version.

Copyright and reuse:

Sussex Research Online is a digital repository of the research output of the University.

Copyright and all moral rights to the version of the paper presented here belong to the individual author(s) and/or other copyright owners. To the extent reasonable and practicable, the material made available in SRO has been checked for eligibility before being made available.

Copies of full text items generally can be reproduced, displayed or performed and given to third parties in any format or medium for personal research or study, educational, or not-for-profit purposes without prior permission or charge, provided that the authors, title and full bibliographic details are credited, a hyperlink and/or URL is given for the original metadata page and the content is not changed in any way.

Vocal tract modelling in fallow deer: are male groans nasalized?

Reby D.^{*}, Wyman M.T.^{*‡}, Frey, R.[#], Charlton B.D.⁺, Dalmont J.P.^{\$} and Gilbert J.^{\$}

^{*}: School of Psychology, University of Sussex, United Kingdom

[‡]: Department of Evolutionary Biology and Environmental Studies, University of Zurich, Switzerland

[#]: Leibniz Institute for Zoo and Wildlife Research (IZW), Berlin, Germany

⁺: Recovery Ecology, San Diego Zoo's Institute for Conservation Research, Escondido, California, United States

^{\$}: Laboratoire d'Acoustique de l'Université du Maine – UMR CNRS, le Mans, France

correspondence: reby@sussex.ac.uk

ABSTRACT

Males of several species of deer have a descended and mobile larynx, resulting in an unusually long vocal tract, which can be further extended by lowering the larynx during call production. Formant frequencies are lowered as the vocal tract is extended, as predicted when approximating the vocal tract as a uniform quarter wavelength resonator. However, formant frequencies in polygynous deer follow uneven distribution patterns, indicating that the vocal tract configuration may in fact be rather complex. We CT-scanned the head and neck region of two adult male fallow deer specimens with artificially extended vocal tracts and measured the cross-sectional areas of the supra-laryngeal vocal tract along the oral and nasal tracts. The CT data was then used to predict the resonances produced by three possible configurations, including the oral vocal tract only, the nasal vocal tract only, or combining both. We found that the area functions from the combined oral and nasal vocal tracts produced resonances more closely matching the formant pattern and scaling observed in fallow deer groans than those predicted by the area functions of the oral vocal tract only or of the nasal vocal tract only. This indicates that the nasal and oral vocal tracts are both simultaneously involved in the production of a nonhuman mammal vocalisation, and suggests that the potential for nasalization in putative oral loud-calls should be carefully considered.

38 INTRODUCTION

39

40 A key objective of mammal vocal communication research is to determine
41 whether the acoustic structure of vocal signals encodes functionally relevant
42 information. To achieve this aim in a given species it is important to
43 understand how vocal signals are produced because any potential acoustic
44 variation is primarily constrained by the biomechanical properties and
45 dimensions of the caller's vocal anatomy (Fitch and Hauser, 2002). While the
46 causal links between vocal production and acoustic variation are well
47 established in human speech (Titze, 1989; Titze, 1994), the biomechanical
48 and physiological sources of acoustic diversity in nonhuman animal signals
49 remain poorly understood. Nonetheless, the generalization of the source-filter
50 theory of human voice production (Fant, 1960) to non-human mammal vocal
51 signals has significantly advanced our understanding of the acoustic structure
52 of mammalian calls in light of their production mechanisms (reviewed by
53 Taylor et al., 2016). According to this theory, voiced vocalizations are the
54 result of a two-stage production process. First, the source signal is generated
55 in the larynx by vocal fold vibration. The rate at which the glottis opens and
56 closes determines the fundamental frequency (F0) of the vocalisation (the
57 main perceptual correlate of the pitch). The source signal is subsequently
58 filtered by the supra-laryngeal vocal tract, whose resonance frequencies
59 shape the spectral envelope of the radiated vocalization, creating broad
60 bands of energy called 'formants' (Fitch, 2000a). Because F0 and formants
61 are produced independently they are subject to separate biomechanical
62 constraints.

63

64 Recent anatomical investigations of mammal supra-laryngeal vocal tracts
65 have revealed an extensive diversity of vocal tract morphology, with e.g.,
66 elongated noses (Frey et al., 2007b), air sacs (Frey et al., 2007a) and
67 descended larynges (Frey and Gebler, 2003), suggesting that vocal tract
68 resonances are under strong selection pressures. Yet, to conclusively
69 determine how such anatomical specialisations affect vocal production
70 requires three-dimensional cineradiography to visualise call-synchronous
71 internal dynamic changes in vocal tract shape and document the position of

oscillating structures during call production (Fitch, 2000b). This approach is however logistically difficult - if not impossible - to perform on large wild animals. An alternative method is to obtain precise vocal tract geometries from cadavers and use this data to generate vocal tract geometries that provide predictions of formant values for multiple vocal tract configurations. Several studies of nonhuman mammals have used this approach to predict the resonance characteristics of air spaces in the upper respiratory tract, showing good concordance with actual formant patterns in species-specific vocalisations (Adam et al., 2013; Carterette et al., 1979, 1984; Gamba et al., 2012; Gamba and Giacoma, 2006b; Koda et al., 2012; Riede et al., 2005). Studies investigating the evolutionary origins of speech have also used vocal tract models to predict the potential articulatory abilities of human ancestors (Boë et al., 2002; Lieberman et al., 1972) as well as non-human primates (Boë et al., 2002; Boë et al., 2017; Fitch et al., 2016). However, attempts at predicting vocal tract resonances from anatomical data remain scant and largely focused on primate species (Gamba et al., 2012; Gamba and Giacoma, 2006a; Koda et al., 2012; Riede et al., 2005), essentially due to the lack of data on vocal tract geometries available for nonhuman terrestrial mammals.

During the autumn breeding season, male fallow deer (*Dama dama*) produce high rates of sexually selected groan vocalisations (Briefer et al., 2010; McElligott and Hayden, 1999). Groans are characterized by a very low F0 and unevenly spaced and modulated formants that obey stereotyped distribution patterns, indicating that they are produced by a consistent, but complex vocal tract shape (Reby et al., 1998; Vannoni and McElligott, 2007). Fallow bucks have a descended and mobile larynx that is retracted towards the sternum during groan production (Fitch and Reby, 2001; McElligott et al., 2006), thereby extending the vocal tract. The effect of vocal tract extension on formant frequencies has been extensively documented in fallow deer (McElligott et al., 2006) and the closely related red deer (Fitch and Reby, 2001; Frey et al., 2012). As the animal extends its vocal tract, formants are lowered until they reach a minimal plateau corresponding to maximal extension, and formant frequency spacing is inversely correlated with the

length of the vocal tract during extension (Fitch and Reby, 2001; McElligott et al., 2006).

Previous attempts at relating formant frequency spacing to vocal tract length have typically modelled the vocal tract as a simple tube of uniform diameter that is closed at the glottis and opened at the mouth (Charlton et al., 2011; Reby and McComb, 2003; Vannoni and McElligott, 2007; Fitch, 1997). Under these assumptions, the length of the vocal tract can be predicted from the formant frequency spacing (and vice-versa) using the equation: $eVTL = c/2 \cdot DF$, where $eVTL$ = estimated vocal tract length, c = the speed of sound in the vocal tract of 350 m/s, and DF is the overall formant frequency spacing measured in the vocalization (Reby and McComb, 2003). Measurements of anatomical oral vocal tract length in adult male fallow deer (taken as the distance from the larynx to the tip of the snout) based on calibrated photographs have produced fully extended vocal tract lengths ranging between 46 cm and 54 cm (McElligott et al., 2006). Yet, the minimum formant spacing (DF) measured in male fallow deer groans varies between 326 Hz to 281 Hz (Vannoni and McElligott, 2007), which, when the vocal tract is modelled as a simple cylindrical tube, corresponds to vocal tract lengths between 54 cm and 62 cm. This overestimation of the vocal tract length from the acoustic data indicates that the animal's vocal tract produces more/lower formants than expected from its anatomical length. Combined with the observation that formants are stereotypically unevenly spaced in groans (McElligott et al., 2006), this suggests the vocal tract configuration during groan production is more complex than previously assumed.

Here we investigate the hypothesis that male fallow deer simultaneously use the oral and nasal vocal tracts as resonating systems during call production, allowing this species to produce a larger number of formants and a more complex formant pattern than predicted by a simple cylindrical tube model. To this end, we performed computed tomography (CT) scans of head-and-neck specimens of male fallow deer to achieve a more detailed description of the complex anatomical structure of the male fallow deer supra-laryngeal vocal tract. The specific aims of this investigation are threefold: 1) to describe the 3-

dimensional geometry of the supra-laryngeal vocal tract in male fallow deer, including the oral and nasal vocal tracts, while the larynx is maximally retracted; 2) to predict the resonance patterns produced by the fully extended vocal tract configuration, simulating the effect of the involvement of the oral vocal tract only, of the nasal vocal tract only, or of the combined oral and nasal vocal tracts on formant patterns; and 3) to compare resonance patterns predicted by each of these configurations with formant patterns observed in actual vocalisations.

MATERIALS AND METHODS

A glossary of the anatomical terms used in this article is provided in the appendix and a schematic representation of the mammalian vocal anatomy is provided in the Electronic Supplementary Material.

Specimen collection

Our measures of vocal tract area functions are based on CT scans from two adult male fallow deer. Male 1 was a 7-year-old buck that died from injuries sustained during a fight with rival males during the breeding season on Oct 20, 2011 in Home Park, London, UK. Male 2 was an 11-year-old buck culled by park staff during annual population control management practices on February 7, 2011 in Richmond Royal Park, London, UK. Both specimens had similar skeletal dimensions: lower mandible length (male 1: 21.0 cm, male 2: 20.3 cm) and lower hind leg length from the calcaneal tuber to the end of the metatarsus (male 1: 31 cm, male 2: 32.5 cm). Head-and-neck specimens of both individuals were obtained by separation between the 2nd and 3rd ribs. Specimens were chilled with ice within 2 hours of death and were frozen at -20° C within 5 hours of death.

Specimen preparation and CT-Scanning

Specimens were thawed, and water was flushed through the oral and nasal vocal tracts to remove debris and fluids and left upright to drain for about 30 minutes before scanning. Specimens were scanned with and without artificially extending the vocal tract. Vocal tract extension was achieved by

maximally pulling the sternothyroid muscle and the trachea towards the sternum and fastening them to the sternum using a string. This recreated a naturalistic configuration of the fully extended vocal tract in male fallow deer.

Specimens were positioned as much as possible in configurations typical of vocalising (see figure 1), although it was not possible to stretch the neck as much as desired (figure 2). The oral cavity was kept open using a block of Styrofoam. This affected the position of the tongue which was pushed backward in an unnatural position in one of the specimens. The detrimental effect on the cross-sectional area measures was moderated by extrapolating the typical position of the tongue from other specimens and anatomical examinations.

Estimation of vocal tract area function

We measured the supra-laryngeal vocal tract area functions (the cross-sectional area at 1 cm steps along the length of the vocal tract, DeBoer and Fitch 2009) using the 3D curved Multi-Planar Representation viewer in Osirix (version 6.0, 64bits for Mac, www.osirix-viewer.com) and following the three-step method described in Kim et al. (2009). First, the oral and nasal vocal tract dorso-ventral midlines were drawn manually using the “3D curved path” tool on a midsagittal section (figure 3). Second, for each vocal tract, cross-sectional areas orthogonal to the midline were produced at 1 cm intervals from the glottis to the lips or nostrils (figure 3). The vocal tract area was then measured in each cross-sectional slice using the closed polygon selection tool to delineate the VT area. Osirix automatically returned the area of the delineated zone (in cm²). Each slice/measure was saved as an image file.

Prediction of vocal tract resonances

The position and amplitude of vocal tract resonances were predicted using the transfer matrix method (Chaigne and Kergomard, 2016), where the tube geometry is approximated as a series of cylindrical elements with variable

cross sections and 1 cm in length. The transfer matrix model is commonly used for modelling acoustic propagation in tube lattices. The method is appropriate when one dimension of the tube is substantially larger than the others, as in most mammalian vocal tracts: below a cut-off frequency F_{co} , ($F_{co} \approx \frac{c}{2D}$, where c is the speed of sound and D the largest transverse dimension) it can be assumed that only plane waves propagate. In this study F_{co} is 4000 Hz as D remains below 4 cm in the fallow deer vocal tract. Assuming linear propagation, the internal acoustic field is perfectly defined by scalar quantities in the frequency domain: the complex amplitudes of the acoustic pressure P and that of the acoustic volume velocity U . For a given cylindrical tube portion of length L and cross sectional area A_o , a 2x2 matrix of complex elements relates vectors $\{P, U\}$ on both sides (input, output) of the cylinder:

$$\begin{pmatrix} P_{in} \\ U_{in} \end{pmatrix} = \begin{pmatrix} \cos kL & i Z_c \sin kL \\ i Z_c^{-1} \sin kL & \cos kL \end{pmatrix} \begin{pmatrix} P_{out} \\ U_{out} \end{pmatrix},$$

where $Z_c = \frac{\rho c}{A_o}$ is the characteristic impedance (where ρ and c are respectively the air density and the speed of sound at body temperature, and $k = \frac{\omega}{c} = \frac{2\pi F}{c}$ is the wave number).

For complex cylindrical geometry, the tube is broken down into smaller elementary cylindrical tubes. If the tube is described by N elementary cylindrical tubes, acoustic pressure and volume flow at the input and output of the tube are related by the matrix equal to the product of the N matrices of the elementary cells:

$$\begin{pmatrix} P_{in} \\ U_{in} \end{pmatrix} = \begin{pmatrix} A & B \\ C & D \end{pmatrix} \begin{pmatrix} P_{out} \\ U_{out} \end{pmatrix}$$

It is thus possible to calculate the input impedance Z_{in} :

$$Z_{in} = \frac{P_{in}}{U_{in}} = \frac{A P_{out} + B U_{out}}{C P_{out} + D U_{out}} = \frac{A Z_{out} + B}{C Z_{out} + D},$$

where $Z_{out} = \frac{P_{out}}{U_{out}}$ is the terminal impedance of the tube. If the tube is open (at the mouth and nostrils for example), Z_{out} is the radiation impedance.

235 If several complex tubes are connected (for example at the branching point of
236 the oral and nasal tracts), there is continuity of the acoustic pressure and
237 conservation of the acoustic volume flow. The particular frequencies where
238 the input impedance magnitude reaches a local maximum, correspond to the
239 vocal tract resonances visible as formants in the spectral acoustic structure of
240 the produced vocalisation.

241 The input parameters are the area functions of the oral and nasal vocal tracts
242 and the branching point of the tracts. The air temperature inside the fallow
243 deer vocal tract, which affects the absolute frequency of predicted resonances
244 (formant frequencies are proportional to the speed of sound in the air and thus
245 to the square root of the absolute temperature) but not their relative frequency
246 distribution, was set to 38°C. The model assumed wall damping of rigid walls
247 and radiation impedance of an open end, un-flanged tube (Chaigne and
248 Kergomard, 2016).

249

250 Resonances were predicted for each male, based on the area functions of
251 three possible configurations:

252 (1) the oral vocal tract only (common laryngopharyngeal tract, oropharynx and
253 oral cavity),

254 (2) the nasal vocal tract only (common laryngopharyngeal tract, nasopharynx
255 and nasal cavities),

256 (3) both the oral and nasal vocal tracts (common laryngopharyngeal tract,
257 oropharynx, oral cavity, nasopharynx, nasal cavities).

258

259 The total cross-sectional areas of both (left and right) nasal cavities were
260 approximated by doubling the cross-sectional areas measured for the left
261 nasal cavity connecting to the left nostril. To approximate the potential effect
262 of the partial opening of the sides of the mouth, we only included half of the
263 portion of the oral cavity that is laterally open. The cross-sectional areas for
264 this portion of the oral cavity were estimated by manually linking the upper lip
265 to the lower lip.

266

267

268 **RESULTS**

269 **Vocal tract anatomy**

270 The potential complete vocal tract is composed of five distinct and connected
271 sections, one of which is paired: 1) the common laryngopharyngeal tract,
272 shared by the oral and nasal vocal tract, between the glottis and the intra-
273 pharyngeal ostium, 2) the oropharynx, from the intra-pharyngeal ostium to the
274 Isthmus faucium (oropharyngeal tract), 3) the oral cavity, from the Isthmus
275 faucium to the mouth opening (oral tract), 4) the nasopharynx, from the intra-
276 pharyngeal ostium to the choanae (nasopharyngeal tract), 5) the paired nasal
277 cavities, from the choanae to the nostrils (nasal tract). The oral vocal tract
278 comprises parts 1,2,3 and the nasal vocal tract parts 1,4,5 (figure 2). The
279 choanae and the Isthmus faucium are located approximately at the same
280 distance from the glottis.

281
282 In the resting configuration (figures 1A, 2A and 4A, B), the pharynx, soft
283 palate and thyrohyoid ligament are relaxed, and the larynx resides at the level
284 of cervical vertebrae 2 and 3, however farther rostrally in male 2 than in male
285 1. Accordingly, the rostral end of the trachea is located 41 cm from the lips in
286 male 1 and 34 cm in male 2. The resting oral vocal tract lengths (glottis to lips)
287 are 36 cm in male 1 and 30 cm in male 2, and the resting nasal vocal tract
288 lengths (glottis to nostrils) are 40 cm in male 1 and 35 cm in male 2 (figures
289 4A, B and 5). The flexible region between the rostral edge of the thyroid
290 cartilage and the base of the epiglottis is relaxed and short (4 cm in both male
291 1 and male 2). Correspondingly, the overall length of the larynx (from cricoid
292 arch to epiglottal tip) is 13 cm in male 1 and 10 cm in male 2. The hyoid
293 apparatus is folded and the distance between the basihyoid and the epiglottis
294 is small (4.5 cm in male 1 and 2.5 cm in male 2). The rostral edge of the intra-
295 pharyngeal ostium (the caudal tip of the palatine velum) is located about 30
296 cm from the lips in male 1 and 25 cm in male 2. The epiglottis is in contact
297 with the intra-pharyngeal ostium or overlaps its rostral edge, so that the
298 laryngeal entrance comes to lie in continuation of the nasopharynx (so-called
299 'intranarial position'). The mouth is mostly closed.

300

301 In the extended phonatory configuration (figures 1B, 2B, 3A, 3D and 4C, D),
302 the pharynx, soft palate and thyrohyoid ligament are maximally extended, and

the larynx resides at the level of cervical vertebrae 4, 5 and 6 in male 1 and 3, 4 and 5 in male 2. Accordingly, the rostral end of the trachea is located approximately 54 cm from the lips in male 1 and 44 cm in male 2. The extended oral vocal tract lengths (glottis to lips) are 48 cm in male 1 and 40 cm in male 2, and the extended nasal vocal tract lengths (glottis to nostrils) are 50 cm in male 1 and 43 cm in male 2 (figures 4C, D and 5). The lengths of the common laryngopharyngeal tract (glottis to intra-pharyngeal ostium) are 12 cm and 9 cm for males 1 and 2, respectively (figures 4C, D and 5). The flexible region between the rostral edge of the thyroid cartilage and the base of the epiglottis is maximally tensed and considerably elongated (7.5 cm in male 1 and 5 cm in male 2). Correspondingly, the overall length of the larynx (from cricoid arch to epiglottal tip) is 15 cm in male 1 and 13 cm in male 2. The hyoid apparatus is maximally unfolded and the thyrohyoid rotated caudally. The distance between the basihyoid and the epiglottis has considerably enlarged, being now 12 cm in male 1 and 7.5 cm in male 2. The rostral edge of the intra-pharyngeal ostium (the caudal tip of the palatine velum) is located approximately 37 cm from the lips in male 1 and 31 cm in male 2. The epiglottis is retracted from the intra-pharyngeal ostium so that the laryngeal entrance is in continuation of both the oropharynx and the nasopharynx. From the intra-pharyngeal ostium onward, the pharyngeal cavity splits into two tubes (the nasopharynx connected to the nasal cavities and the oropharynx connected to the oral cavity) completely separated by the soft palate (velum). The mouth is opened for vocalizing.

326

327

328 **Cross-sectional areas**

329 The cross sectional areas measured along each of the male specimen's vocal
330 tracts are shown in figure 5. The area functions from the glottis (right) towards
331 the lips and nostrils (left) are highly comparable between the two specimens.
332 Longitudinally, the choanae and the Isthmus faucium are located about 25-30
333 cm (male 1) and 20-25 cm (male 2) rostral to the glottis, respectively (figure
334 5).

335 The decrease of the cross-sectional area from the glottis towards the intra-
336 pharyngeal ostium is a consequence of the large larynx of male fallow deer.

337 Its considerable dorsoventral height causes a relatively large intra-laryngeal
338 cross-sectional area at the glottis (figure 3D cross-section 1). From the intra-
339 pharyngeal ostium the cross-sectional area of the nasopharynx increases
340 towards the choanae and, similarly, the cross-sectional area of the
341 oropharynx increases towards the Isthmus faucium. Choanae and Isthmus
342 faucium mark the rostral end of the pharynx, i.e. the transition from the
343 nasopharynx to the nasal cavities and from the oropharynx to the oral cavity,
344 respectively. The gradual, mostly uniform increase in cross-sectional area,
345 from the intra-pharyngeal ostium towards the rostral end of the pharynx,
346 reflects the basic funnel-shape of the pharynx, narrowest at its connection to
347 the larynx and widest at its connection to the skull and the oral cavity. From
348 the choanae to the nostrils there is an overall decrease of cross-sectional
349 area as a consequence of the narrowing of the nasal cavities towards the
350 muzzle. The particular decrease of cross-sectional area at around 42 cm in
351 male 1 and at around 37 cm in male 2 comes from the ventral nasal conchae,
352 which narrow the nasal cavities by their extensive, scrolled osseous lamellae
353 (figure 3D cross-section 3). From the Isthmus faucium to the lips the cross-
354 sectional area initially increases and then decreases. In between is a
355 particular decrease at around 39 cm in male 1 and around 33 cm in male 2.
356 The initial increase represents the caudal end of the oral cavity between the
357 Isthmus faucium and the root of the tongue and the final decrease the rostral
358 end of the oral cavity between the lingual fossa and the lips. The intermediate
359 decrease in cross-sectional area results from the lingual torus, an elevation of
360 the tongue in ruminants, which considerably narrows the middle oral cavity.
361 When the mouth is opened and the lower jaw depressed for groan emission
362 the cross-sectional areas of the (then funnel-shaped) oral cavity will increase
363 accordingly in direction towards the lips.

364

365

366 **Predicted Vocal tract resonances**

367 The vocal tract resonances predicted from the vocal tract area functions of
368 male 1 and male 2 and corresponding to the three possible configurations are
369 presented in figure 6. F1 predicted by the combined oral and nasal vocal
370 tracts is in intermediate position between the F1 predicted using the oral vocal

tract only, or the nasal vocal tract only. F2 and F3 predicted by the combined oral and nasal vocal tracts corresponds to the F2 predicted by the nasal vocal tract only, and to the F2 predicted by the oral vocal tract only. F4 and F5 predicted by the combined oral and nasal vocal tracts corresponds to the F3 predicted by the nasal vocal tract only, and to the F3 predicted by the oral vocal tract only (figure 6, table 1).

The centre frequencies of each predicted formant are reported in table 1. The models using both oral and nasal vocal tracts predict much lower formants overall (average formant spacing of 255 Hz) than models using the oral vocal tract only (average formant spacing of 446 Hz) or models using the nasal vocal tract only (average formant spacing of 358 Hz).

Table 1: Predicted centre frequencies for formants F1 to F5 (Hz) and estimated formant spacing (DF) for the different vocal tract configurations for males 1 and 2.

configuration	male	F1	F2	F3	F4	F5	DF
oral vocal tract only	1	249	494	1044	1352	1938	410
	2	305	581	1238	1629	2238	482
nasal vocal tract only	1	175	359	771	1166	1534	328
	2	194	505	981	1426	1712	388
combined oral and nasal vocal tracts	1	223	365	495	776	1060	227
	2	255	503	582	992	1302	283

Comparison with acoustic observations

Figure 7 plots the average centre frequencies of the first five formants observed in groans from 16 adult fallow deer males (reported in Vannoni and McElligott, 2007, see table 2) against the resonances predicted by our three

vocal tract models. The resonances predicted by a vocal tract including both the oral and nasal vocal tracts are a better fit to the observed formants than those predicted by using the oral vocal tract or the nasal vocal tract only: the slope of the regression line is closer to 1 (indicating a better fit of the scaling of the resonances), and R^2 is also higher (indicating a better fit of the pattern of the resonances). Examination of the regression slopes in figure 7 shows that while model 3 (combined oral and nasal vocal tracts) underestimates the formant frequency spacing by 9%, model 1 (oral vocal tract only) overestimates DF by 37% and model 2 (nasal vocal tract only) overestimates DF by 23%. Separate correlations for male 1 and male 2 are given in the Electronic Supplementary Material.

403

Table 2: Average centre frequencies for formants F1 to F5 (Hz) and average estimated formant spacing (DF) at maximal vocal tract extension from 16 adult males (Vannoni & McElligott 2007).

Formant:	F1	F2	F3	F4	F5	DF
Average centre	208.5	414.3	575.2	1060.2	1265.9	300.6
frequency (Hz) \pm SE	± 2.0	± 1.9	± 3.3	± 2.9	± 3.2	± 0.8
Minimum centre	152	329	457	966	1170	281
frequency (Hz)						
Maximum centre	263	496	677	1149	1371	326
frequency (Hz)						

407

408

409 DISCUSSION

410

In this study, the artificially extended vocal apparatuses of two adult male fallow deer were CT-scanned, and the cross-sectional areas of the complete supra-laryngeal vocal tract (common laryngopharyngeal tract, oropharynx,

414 oral cavity, nasopharynx and nasal cavities) of both specimens were
415 measured along the oral and nasal vocal tracts. We then used this data to
416 model resonance patterns produced by these supra-laryngeal cavities
417 including the oral vocal tract only, the nasal vocal tract only or the combined
418 oral and nasal vocal tracts. We found that the configuration combining the oral
419 and nasal vocal tract geometries produced a resonance pattern which more
420 closely matches the formants observed in fallow deer groans, both in term of
421 formant frequency pattern and in term of formant frequency scaling.

422

423 The formants observed in the groans of fallow deer (Briefer et al., 2010;
424 McElligott and Hayden, 1999) and more generally in the sexually-selected
425 calls of male polygynous deer with extensible vocal tracts (Fitch and Reby,
426 2001; Passilongo et al., 2013; Reby and McComb, 2003; Reby et al., 2016)
427 obey stereotyped, uneven formant patterns incompatible with a vocal tract
428 consisting of a simple linear tube. More specifically, in both fallow deer groans
429 (McElligott et al., 2006) and red deer roars (Reby and McComb, 2003) the
430 second and third formants are close to one another and the fourth formant is
431 higher, leaving a gap between the third and fourth formant. Our simulations
432 combining both the oral and nasal vocal tracts predict this pattern.
433 Comparison of the models suggests that formants two and four of fallow deer
434 groans are affiliated to the nasal vocal tract while formants three and five are
435 affiliated to the oral vocal tract.

436

437 In terms of frequency scaling, our predictions resolve the aforementioned
438 mismatch between apparent vocal tract lengths estimated from formant
439 frequencies measured in fallow deer groans and actual anatomical vocal tract
440 length derived from photogrammetric and anatomical data. Presumably this is
441 because the inclusion of formants affiliated to the nasal vocal tract led to an
442 overestimation of apparent vocal tract length in previous studies modelling the
443 fallow deer vocal tract as a single uniform tube. Indeed, previous
444 investigations of apparent vocal tract length (i.e. vocal tract length estimated
445 from formant frequencies) in polygynous deer with descended and mobile
446 larynges (Corsican deer: Kidjo et al., 2008; fallow deer: McElligott et al., 2006;
447 Mesola deer: Passilongo et al., 2013; red deer: Reby and McComb, 2003)

448 have modelled the vocal tract as a linear tube with constant cross-section
449 closed at one end (glottis) and open at the other (mouth), and excluded the
450 involvement of the nasal vocal tract for loud calls produced with an open
451 mouth. While these succeeded at characterizing inter-individual differences in
452 formant frequency spacing (Kidjo et al., 2008; Vannoni and McElligott, 2007),
453 apparent vocal tract length and thus body size (Reby and McComb, 2003;
454 Vannoni and McElligott, 2008), they probably yielded over-estimations of the
455 anatomical vocal tract length.

456

457 The inclusion of nasal resonances in future models should allow for better
458 estimations of apparent vocal tract length from recorded mating calls in these
459 species, thereby potentially enhancing the reliability of bioacoustics tools
460 aimed at assessing body size from vocalisations for research, conservation or
461 wildlife management purposes.

462

463 Taken together our observations strongly suggest that the nasal cavity and
464 oral cavity are both simultaneously involved in the vocal production of fallow
465 deer groans. This involvement of the nasal vocal tract due to the non-closure
466 of the intra-pharyngeal ostium during vocal tract extension maybe widespread
467 in species with a permanently descended larynx and extensible vocal tract
468 (such as other polygynous deer and e.g. goitred gazelles), but also occur in
469 species where callers lower their larynx temporarily for the production of oral
470 (rather than nasal) calls. We suggest that the potential for nasalization of
471 putative oral loud calls should be carefully examined across terrestrial
472 mammals.

473

474 The role of nasal cavities in acoustic output has been investigated in humans
475 using anatomical scans, area functions, vocal tract modeling, and/or acoustic
476 analysis (Dang et al., 1994; Feng and Castelli, 1996; Hattori and Fujimura,
477 1958; Pruthi et al., 2007; Story, 2005). Compared to modulation of the oral
478 vocal tract, nasalization plays a relatively minor role in human speech
479 variation and is often left out of vocal models. However, models that include
480 coupling between the nasal and oral cavity can result in transfer functions that
481 more closely match recorded acoustic output (Dang et al., 1994; Feng and

482 Castelli, 1996). The effects of nasalization are strongest in the lower
483 frequencies (Feng and Castelli, 1996; Pruthi et al., 2007) and include the
484 addition of low frequency formant peaks as observed here in fallow deer
485 groans. Nasal coupling has also been suggested as a likely mechanism for
486 the addition of low spectral peaks in Diana monkey alarm calls (Riede and
487 Zuberbuhler, 2003).

488

489 There are obvious limitations to this investigation. Our dead specimens were
490 scanned in artificial positions constrained by the dimensions of the CT-
491 scanner, and thus only approximate the natural postures of live animals
492 during vocalising. Moreover, the vocal tracts were artificially extended. The
493 geometries are thus approximations of the vocal tract of live animals during
494 vocalizing, and do not account for internal adjustments such as, e.g., the
495 possible contribution of palatopharyngeal muscles. Future investigations could
496 involve performing several scans involving different combinations of varying
497 head/neck angle, extent of the laryngeal descent, or mouth opening; or
498 perform simulations of these parameters (Gamba et al., 2012; Gamba and
499 Giacomini, 2006b). Using a larger sample of specimens would also allow the
500 assessment of inter-individual variation, including the effect of age or size.

501

502 Formants frequencies are known to provide cues to the caller's body size in
503 fallow deer groans and red deer roars, due to a close correlation between
504 formant frequency spacing and body size (McElligott et al., 2006; Reby and
505 McComb, 2003), and are used by male and female receivers to assess rivals
506 and potential mates during the breeding season (Charlton et al., 2008a;
507 Charlton et al., 2007; Charlton et al., 2008b; Pitcher et al., 2015; Reby et al.,
508 2005). The descended larynx and extensible vocal tract of fallow and red deer
509 males (and some other species) are therefore considered to be adaptations
510 that allow callers to maximise the acoustic impression of their body size
511 conveyed to receivers (the "size exaggeration hypothesis" Fitch and Reby,
512 2001; Ohala, 1984). Our investigations show that the involvement of the nasal
513 vocal tract adds additional formants to the lower part of the spectrum, which
514 increases formant density (decreasing formant spacing), and may make the
515 caller sound larger when compared to oral or nasal only calls. Similar

functional explanations have been suggested for the evolution of air sacs (de Boer, 2009; Harris et al., 2006), which also increase formant density by adding resonances.

In conclusion, we contend that, while expensive and technically challenging, using 3-dimensional CT scanning to predict vocal tract resonances can greatly assist the interpretation of formant patterns in mammal vocalizations. We suggest that similar approaches could be generalized to the study of vocal tract resonances in other terrestrial mammals.

Appendix: Glossary of Anatomical Terms used in this paper (based on Constantinescu & Schaller 2012 and own descriptions)

Basihyoid: unpaired, most ventral, transverse component of hyoid apparatus intercalated between the paired suspension from the skull and the paired arms to the larynx.

Choanae: the 'internal nares', i.e. the two openings at the caudal end of the nasal cavity, where the paired nasal meatuses lead into the nasopharynx.

Cricoid cartilage: the most caudal, ring-shaped cartilage of the larynx that is attached to the trachea; it consists of a dorsal plate and a ventral arch.

Epiglottis: the most rostral cartilage of the larynx; during quiet breathing it has a so-called intranarial position, i.e. it protrudes dorsally, through the intra-pharyngeal ostium, into the nasopharynx; during an open-mouth call the larynx is withdrawn from the intra-pharyngeal ostium so that it is now positioned in the oropharynx.

Glottis: forms the vocal source of the larynx; it consists of the two vocal folds, ventral parts of the arytenoid cartilages and the vocal cleft in between the vocal folds; regarding the laryngeal cavity it is positioned between the laryngeal vestibule rostrally, and the infraglottic cavity caudally.

Hyoid apparatus: a framework of small rod-like bones connecting dorsally to the base of the skull, rostrally to the tongue, and caudally to the larynx; it consists of 3 components: the arms of the paired dorsal part flank the pharynx on both sides and suspend the entire hyoid apparatus from the skull base, it

550 consists of several parts on both sides termed (dorsal to ventral):
551 tympanohyoid, stylohyoid, epihyoid, ceratohyoid; the arms of the paired
552 caudal part connect to the larynx (in fallow deer via the two thyrohyoid
553 ligaments); it consists of one element per side termed thyrohyoid; the
554 unpaired, transverse ventral part connects the two paired structures thereby
555 forming a larger U-shaped fork for suspension from the skull dorsally and a
556 smaller U-shaped fork for connection to the larynx caudally.

557 **Intra-pharyngeal ostium:** opening in the soft palate, creating a passage
558 between nasopharynx and oropharynx; it is bordered by the palatopharyngeal
559 muscle that can constrict the intra-pharyngeal ostium.

560 **Isthmus faucium:** narrow short passage between the mouth cavity and the
561 oropharynx, bounded by the soft palate dorsally, the tongue ventrally, and the
562 palatoglossal arch (a symmetrical, dorsoventral mucosa fold between soft
563 palate and tongue) laterally.

564 **Laryngeal entrance:** rostral entrance to the larynx, bounded by the epiglottis,
565 the aryepiglottic folds and the corniculate processes of the arytenoid
566 cartilages.

567 **Nasopharynx:** nasal part of the pharynx, dorsal to the soft palate; it extends
568 from the choanae to the intrapharyngeal ostium.

569 **Oropharynx:** oral part of the pharynx, ventral to the soft palate; it extends
570 from the isthmus faucium to the base of the epiglottis.

571 **Pharynx:** musculomembraneous cross way of the respiratory and digestive
572 tracts between the oral and nasal cavities rostrally, and the oesophagus and
573 larynx caudally; for the sake of simplicity, and in contrast to textbooks, the
574 pharynx is here not subdivided in 3 parts (nasal, oral and laryngeal) but only
575 in 2 parts (nasal and oral).

576 **Soft palate:** the palatine velum or soft palate, is a soft tissue structure that is
577 laterally fused to the pharyngeal walls; it completely separates naso- and
578 oropharynx, except at the intra-pharyngeal ostium, which represents the only
579 communication between Naso- and Oropharynx; as the pharynx, it extends
580 from the choanae to the larynx.

581 **Thyrohyoid:** paired caudal element of the hyoid apparatus that, together with
582 the basihyoid, forms the smaller U-shaped fork for establishing the connection
583 between the hyoid apparatus and the larynx.

584 **Thyrohyoid ligament:** replaces the usual thyrohyoid articulation of most
585 mammals by a ligamentous connection between the caudal tip of the
586 thyrohyoid bone (of the hyoid apparatus) and the rostral horn of the thyroid
587 cartilage.

588 **Thyroid cartilage:** The most superficial and largest cartilage of the larynx,
589 unpaired, its two lateral laminae are ventrally fused and enclose most of the
590 laryngeal cavity in between them; its rostral horn connects the larynx to the
591 thyrohyoid of the hyoid apparatus, its caudal horn articulates with the cricoid
592 cartilage in the cricothyroid articulation.

593 **Trachea:** Windpipe, connecting the lungs to the larynx, extends from its
594 bifurcation into the main bronchi caudally to the cricoid cartilage of the larynx
595 rostrally.

596

597 **Acknowledgements**

598 We thank John Bartram, John Comfort, and Paul Douglas at the London
599 Royal Parks for their help obtaining the specimens. We are also very grateful
600 to Jan Bush and the amazing staff at CISC for facilitating the production of the
601 CT-Scans.

602

603 **Competing interests**

604 The authors declare no competing or financial interests.

605

606 **Author contributions**

607 D.R. supervised the research. M.T.W., R.F. and D.R. performed the
608 anatomical and imaging investigations. J.G., J-PD. and D.R. performed the
609 acoustical modelling. D.R., M.T.W., R.F., B.D.C., J-PD. and J.G. wrote the
610 manuscript.

611

612 **Funding**

613 J.G. was supported by a Projet International de Coopération Scientifique grant
614 reference 6188 from Centre National de la Recherche Scientifique. DR was
615 supported by an invited professorship from Le Mans Université. MW was

616 supported by a grant from US National Science Foundation International
617 Research Fellowship (grant number 0908569) and an award from the
618 Systematics Research Fund.

619

620 **Data availability**

621 Supporting data and scripts for predicting vocal tract resonances are available
622 on request from the corresponding author.

623

624 **Figure Legends**

625

626 **Figure 1. Fallow deer buck in a pre-groaning posture (A) and in a**
627 **groaning posture (B) during the annual rut.** In (A) the neck is not extended,
628 the larynx is in its resting position and the mouth is closed. In (B) the neck is
629 extended, the larynx retracted, and the mouth is opened (no lip rounding).
630 Single frames from a video by D. Belton ©.

631

632 **Figure 2. CT-based 3-D reconstructions of male 1.** (A): larynx and hyoid
633 apparatus in pre-groan (resting) position. (B): larynx and hyoid apparatus in a
634 groaning position at full artificial extension of the vocal tract. The larynx
635 position is shifted caudally by approximately 12 cm. ochre: common
636 laryngopharyngeal tract; green: oropharynx and oral cavity; blue: nasopharynx
637 and nasal cavities.

638

639 **Figure 3. Multi-Planar Representation of a CT scan of male 1 illustrating**
640 **the methodology for measuring the vocal tract area function at maximal**
641 **artificial extension.** (A): manually drawn dorso-ventral and transverse
642 midline through the oral vocal tract; (B): sampling transverse sections along
643 the virtually stretched, un-curved oral vocal tract in 1 cm steps; (C): three
644 examples of the obtained cross-sections highlighting the respective contours
645 of the oral vocal tract in green. (D): Sagittal section of the oral vocal tract (left,
646 midline in red), the nasal vocal tract (right, midline in green) and
647 representative cross-sections at the level of the glottis (1), of the naso- and
648 oro-pharynx separated by the soft palate (2) and of the nasal cavities (3).

649

650 **Figure 4. Midsagittal slices of CT scans of males 1 and 2 with the larynx**
651 **and vocal tract in a pre-groaning (resting) position (A and B) and in a**
652 **groaning position with the larynx maximally retracted and the vocal tract**
653 **fully extended (C and D).** C1 – C7, T1 = cervical vertebrae 1-7, first thoracic
654 vertebra; Cart. aryt. = arytenoid cartilage; Cart. cric. = cricoid cartilage; Cart.
655 thyr. = thyroid cartilage; Cav. oris = oral cavity; Choan. = choanae (caudal
656 nasal apertures, internal nares); Epigl. = epiglottis; Glott. = glottis; Ling. =
657 tongue; Nasophar. = nasal part of pharynx; Nostr. = nostrils (rostral nasal
658 apertures, external nares); Orophar. = oral part of pharynx; Ost. intrphar. =
659 intra-pharyngeal ostium (IPO); Palat. dur. = hard palate; Palat. mol. = soft
660 palate ('velum'); Trach. = trachea; o = rostral tip of sternal manubrium;
661 asterisk: position of the basihyoid. Compared to the resting state, the
662 elongation of the oral and nasal vocal tract is 33% in male 1 (A, C) and 25% in
663 male 2 (B, D). Scale: 10 cm

664
665 **Figure 5.** Estimation of oral and nasal vocal tract cross-sectional areas in the
666 maximally extended state, proceeding from right to left, in male 1 (A) and
667 male 2 (B).

668
669 **Figure 6. Predicted resonances for the three possible vocal tract**
670 **configurations of groan production in male 1 (A) and male 2 (B).** Red
671 lines: combined oral and nasal vocal tracts; green lines: nasal vocal tract only;
672 blue lines: oral vocal tract only. The resonance pattern produced by the
673 combined oral and nasal vocal tracts is more similar to the observed formants
674 in fallow deer groans than the resonance patterns of either oral or nasal vocal
675 tract alone.

676
677 **Figure 7. Correlations between resonances observed in male fallow deer**
678 **groans (y axis) and resonances predicted from vocal tract geometries of**
679 **scanned specimens (x axis).** Predicted resonances are the average centre
680 frequencies of the first 5 peaks predicted by the cross-sectional areas of the
681 vocal tract of male 1 and 2 including the oral vocal tract only (blue line), the
682 nasal vocal tract only (green line), or both the oral and nasal vocal tracts (red
683 line). The regression slopes inform the fit of the scaling (formant spacing) of

the observed resonances to the predicted resonances. The values of R^2 provide the fit of the pattern of the observed resonances to the predicted resonances.

References

- Adam, O., Cazau, D., Gandilhon, N., Fabre, B., Laitman, J. T. and Reidenberg, J. S. (2013). New acoustic model for humpback whale sound production. *Applied Acoustics* **74**, 1182-1190.
- Boë, L.-J., Heim, J., Honda, K. and Maeda, S. (2002). The potential Neandertal vowel space was as large as that of modern humans. *Journal of phonetics* **30**, 465-484.
- Boë, L.-J., Berthommier, F., Legou, T., Captier, G., Kemp, C., Sawallis, T. R., Beckers, Y., Rey, A. and Fagot, J. (2017). Evidence of a vocalic proto-system in the baboon (*Papio papio*) suggests pre-hominin speech precursors. *PLoS ONE* **12**, e0169321.
- Briefer, E., Vannoni, E. and McElligott, A. G. (2010). Quality prevails over identity in the sexually selected vocalisations of an ageing mammal. *BMC Biology* **8**, 1-15.
- Carterette, E. C., Shipley, C., and Buchwald, J. (1979). Linear prediction theory of vocalization in cat and kitten, in *Frontiers in Speech Communication Research*, edited by B. Lindblom, and S. Ohman (Academic Press, New York), pp. 245-257.
- Carterette, E. C., Shipley, C., and Buchwald, J. S. (1984). On synthesizing animal speech: The case of the cat," in *Electronic speech synthesis : techniques, technology, and applications*, edited by G. Bristow (McGraw-Hill, New York), pp. 292-302.
- Chaigne, A. and Kergomard, J. (2016). *Acoustics of musical instruments* New York: Springer.
- Charlton, B., Ellis, W., McKinnon, A., Cowin, G., Brumm, J., Nilsson, K. and Fitch, W. (2011). Cues to body size in the formant spacing of male koala (*Phascolarctos cinereus*) bellows: honesty in an exaggerated trait. *Journal of Experimental Biology* **214**, 3414-3422.
- Charlton, B., McComb, K. and Reby, D. (2008a). Free-ranging red deer hinds show greater attentiveness to roars with formant frequencies typical of young males. *Ethology* **114**, 1023-1031.
- Charlton, B., Reby, D. and McComb, K. (2007). Female red deer prefer the roars of larger males. *Biology Letters* **3**, 382-385.
- Charlton, B., Reby, D. and McComb, K. (2008b). Effect of combined source (F0) and filter (formant) variation on red deer hind responses to male roars. *Journal of the Acoustical Society of America* **123**, 2936-2943.
- Constantinescu, G.M., Schaller, O. (2012). *Illustrated Veterinary Anatomical Nomenclature*, 3rd revised edition, Enke Verlag, Stuttgart, 620 pp.
- Dang, J. W., Honda, K. and Suzuki, H. (1994). Morphological and acoustical analysis of the nasal and the paranasal cavities. *Journal of the Acoustical Society of America* **96**, 2088-2100.

730 **de Boer, B.** (2009). Acoustic analysis of primate air sacs and their effect
731 on vocalization. *The Journal of the Acoustical Society of America* **126**, 3329–3343.

732 **Fant, G.** (1960). Acoustic Theory of Speech Production. The Hague:
733 Mouton.

734 **Feng, G. and Castelli, E.** (1996). Some acoustic features of nasal and
735 nasalized vowels: A target for vowel nasalization. *Journal of the Acoustical Society*
736 *of America* **99**, 3694-3706.

737 **Fitch, W. T.** (1997). Vocal tract length and formant frequency dispersion
738 correlate with body size in rhesus macaques. *Journal of the Acoustical Society of*
739 *America* **102**, 1213-1222.

740 **Fitch, W. T.** (2000a). The evolution of speech: a comparative review.
741 *Trends in Cognitive Sciences* **4**, 258-267.

742 **Fitch, W. T.** (2000b). The phonetic potential of nonhuman vocal tracts:
743 Comparative cineradiographic observations of vocalizing animals. *Phonetica* **57**,
744 205-218.

745 **Fitch, W. T., de Boer, B., Mathur, N. and Ghazanfar, A. A.** (2016).
746 Monkey vocal tracts are speech-ready. *Science Advances* **2**, e1600723-e1600723.

747 **Fitch, W. T. and Hauser, M. D.** (2002). Unpacking "Honesty": Generating
748 and extracting information from acoustic signals. In *Animal Communication*, eds.
749 A. Megala-Simmons and A. Popper), pp. 65-137. Berlin: Springer-Verlag.

750 **Fitch, W. T. and Reby, D.** (2001). The descended larynx is not uniquely
751 human. *Proceedings of the Royal Society of London, Series B: Biological Sciences*
752 **268**, 1669-1675.

753 **Frey, R. and Gebler, A.** (2003). The highly specialized vocal tract of the
754 male Mongolian gazelle (*Procapra gutturosa* Pallas, 1777 - *Mammalia, Bovidae*).
755 *Journal of Anatomy* **203**, 451-471.

756 **Frey, R., Gebler, A., Fritsch, G., Nygren, K. and Weissengruber, G.**
757 (2007a). Nordic rattle: the hoarse vocalization and the inflatable laryngeal air sac
758 of reindeer (*Rangifer tarandus*). *Journal of Anatomy* **210**, 131-159.

759 **Frey, R., Volodin, I. and Volodina, E.** (2007b). A nose that roars:
760 anatomical specializations and behavioural features of rutting male saiga. *Journal*
761 *of Anatomy* **211**, 717-736.

762 **Frey, R., Volodin, I., Volodina, E., Carranza, J. and Torres-Porras, J.**
763 (2012). Vocal anatomy, tongue protrusion behaviour and the acoustics of rutting
764 roars in free-ranging Iberian red deer stags (*Cervus elaphus hispanicus*). *Journal*
765 *of Anatomy* **220**, 271-292.

766 **Gamba, M., Friard, O. and Giacoma, C.** (2012). Vocal tract morphology
767 determines species-specific features in vocal signals of lemurs (*Eulemur*).
768 *International Journal of Primatology* **33**, 1453-1466.

769 **Gamba, M. and Giacoma, C.** (2006a). Vocal tract configurations and
770 formant pattern variation in ruffed lemurs vocal production. In *Proceedings of*
771 *the ICPV 2006, The 5th International Conference on Voice Physiology and*
772 *Biomechanics, Variations across Cultures and Species.*, pp. 38-41. Tokyo, Japan.

773 **Gamba, M. and Giacoma, C.** (2006b). Vocal tract modeling in a prosimian
774 primate: the black and white ruffed lemur. *Acta Acustica United With Acustica* **92**,
775 749-755.

776 **Harris, T. R., Fitch, W. T., Goldstein, L. M. and Fashing, P. J.** (2006).
777 Black and white colobus monkey (*Colobus guereza*) roars as a source of both
778 honest and exaggerated information about body mass. *Ethology* **112**, 911-920.

779 **Hattori, S. and Fujimura, O.** (1958). Nasalization of vowels in relation to
780 nasals. *Journal of the Acoustical Society of America* **30**, 267-274.

781 **Kidjo, N., Cargnelutti, B., Charlton, B. D., Wilson, C. and Reby, D.**
782 (2008). Vocal behaviour in the endangered Corsican deer: description and
783 phylogenetic implications. *Bioacoustics* **18**, 159-181.

784 **Koda, H., Nishimura, T., Tokuda, I. T., Oyakawa, C., Nihonmatsu, T.**
785 **and Masataka, N.** (2012). Soprano singing in gibbons. *American Journal of*
786 *Physical Anthropology* **149**, 347-355.

787 **Lieberman, P., Crelin, E. S. and Klatt, D. H.** (1972). Phonetic ability and
788 related anatomy of the newborn and adult human, Neanderthal man, and the
789 chimpanzee. *American Anthropologist* **74**, 287-307.

790 **McElligott, A. G., Birrer, M. and Vannoni, E.** (2006). Retraction of the
791 mobile descended larynx during groaning enables fallow bucks (*Dama dama*) to
792 lower their formant frequencies. *Journal of Zoology* **270**, 340-345.

793 **McElligott, A. G. and Hayden, T. J.** (1999). Context-related vocalization
794 rates of fallow bucks, *Dama dama*. *Animal Behaviour* **58**, 1095-1104.

795 **Ohala, J. J.** (1984). An ethological perspective on common cross-language
796 utilization of F0 of voice. *Phonetica* **41**, 1-16.

797 **Passilongo, D., Reby, D., Carranza, J. and Apollonio, M.** (2013). Roaring
798 high and low: composition and possible functions of the Iberian stag's vocal
799 repertoire. *PLoS ONE* **8**, e63841.

800 **Pitcher, B. J., Briefer, E. F. and McElligott, A. G.** (2015). Intrasexual
801 selection drives sensitivity to pitch, formants and duration in the competitive
802 calls of fallow bucks. *BMC Evolutionary Biology* **15**, 149.

803 **Pruthi, T., Espy-Wilson, C. Y. and Story, B. H.** (2007). Simulation and
804 analysis of nasalized vowels based on magnetic resonance imaging data. *Journal*
805 *of the Acoustical Society of America* **121**, 3858-3873.

806 **Reby, D., Joachim, J., Lauga, J., Lek, S. and Aulagnier, S.** (1998).
807 Individuality in the groans of fallow deer (*Dama dama*) bucks. *Journal of Zoology*
808 **245**, 79-84.

809 **Reby, D. and McComb, K.** (2003). Anatomical constraints generate
810 honesty: acoustic cues to age and weight in the roars of red deer stags. *Animal*
811 *Behaviour* **65**, 519-530.

812 **Reby, D., McComb, K., Cargnelutti, B., Darwin, C., Fitch, W. T. and**
813 **Clutton-Brock, T. H.** (2005). Red deer stags use formants as assessment cues
814 during intrasexual agonistic interactions. *Proceedings of the Royal Society of*
815 *London, Series B: Biological Sciences* **272**, 941-947.

816 **Reby, D., Wyman, M. T., Frey, R., Passilongo, D., Gilbert, J., Locatelli, Y.**
817 **and Charlton, B. D.** (2016). Evidence of biphonation and source-filter
818 interactions in the bugles of male North American wapiti (*Cervus canadensis*).
819 *Journal of Experimental Biology* **219**, 1224-1236.

820 **Riede, T., Bronson, E., Hatzikirou, H. and Zuberbuhler, K.** (2005).
821 Vocal production mechanisms in a non-human primate: morphological data and
822 a model. *Journal of Human Evolution* **48**, 85-96.

823 **Riede, T. and Zuberbuhler, K.** (2003). The relationship between
824 acoustic structure and semantic information in Diana monkey alarm
825 vocalization. *Journal of the Acoustical Society of America* **114**, 1132-1142.

826 **Story, B. H.** (2005). A parametric model of the vocal tract area function
827 for vowel and consonant simulation. *Journal of the Acoustical Society of America*
828 **117**, 3231-3254.

829 **Taylor, A., Charlton, B. D. and Reby, D.** (2016). Vocal production by
830 terrestrial mammals: source, filter and function. In *Vertebrate sound production*
831 *and acoustic communication*, eds. R. A. Suthers W. T. Fitch R. R. Fay and A.
832 Popper). Berlin: Springer International Publishing.

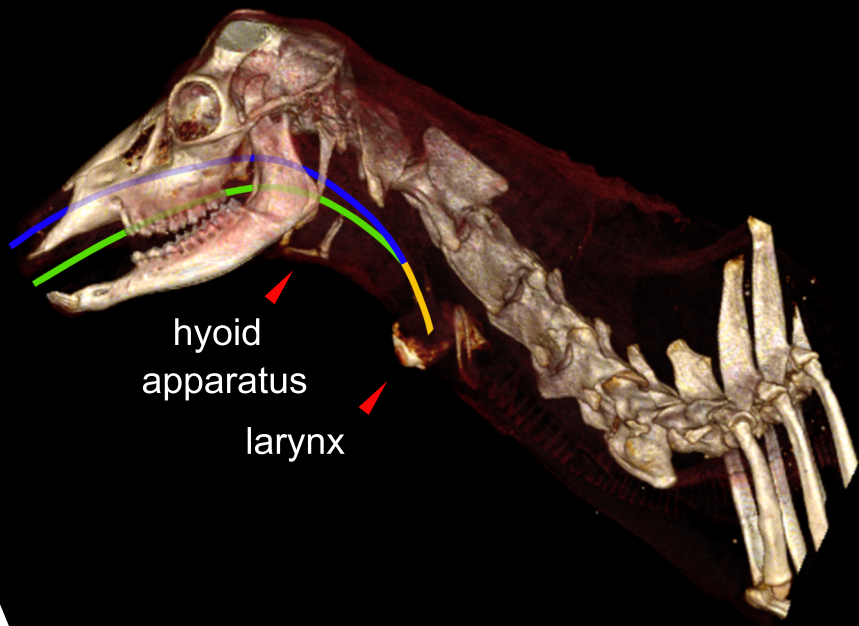
833 **Titze, I. R.** (1989). Physiologic and acoustic differences between male and
834 female voices. *Journal of the Acoustical Society of America* **85**, 1699-1707.

835 **Titze, I. R.** (1994). Principles of Voice Production. Englewood Cliffs, New
836 Jersey: Prentice Hall.

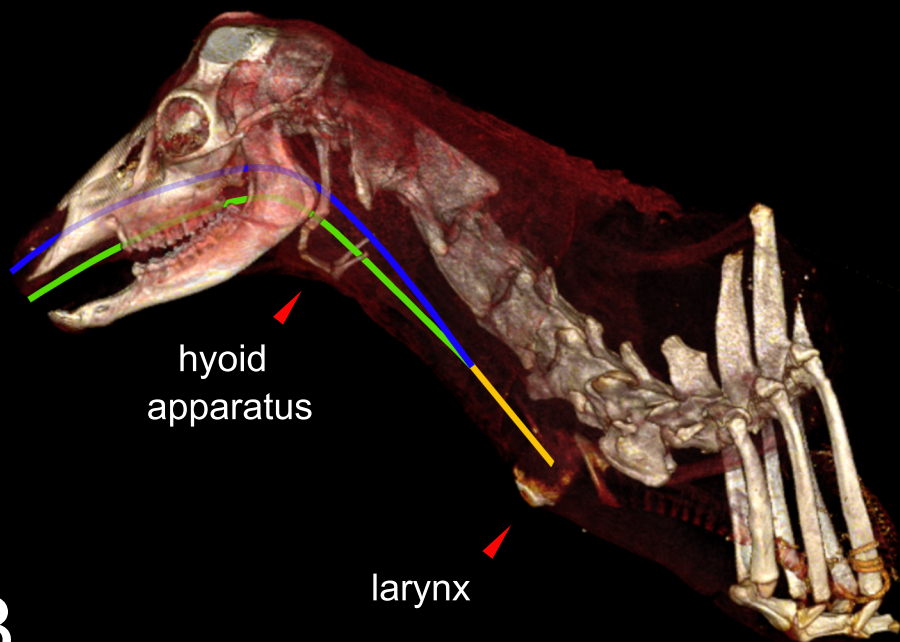
837 **Vannoni, E. and McElligott, A. G.** (2007). Individual acoustic variation in
838 fallow deer (*Dama dama*) common and harsh groans: a source-filter theory
839 perspective. *Ethology* **113**, 223-234.

840 **Vannoni, E. and McElligott, A. G.** (2008). Low frequency groans indicate
841 larger and more dominant fallow deer (*Dama dama*) males. *PLoS ONE* **3**, e3113.
842

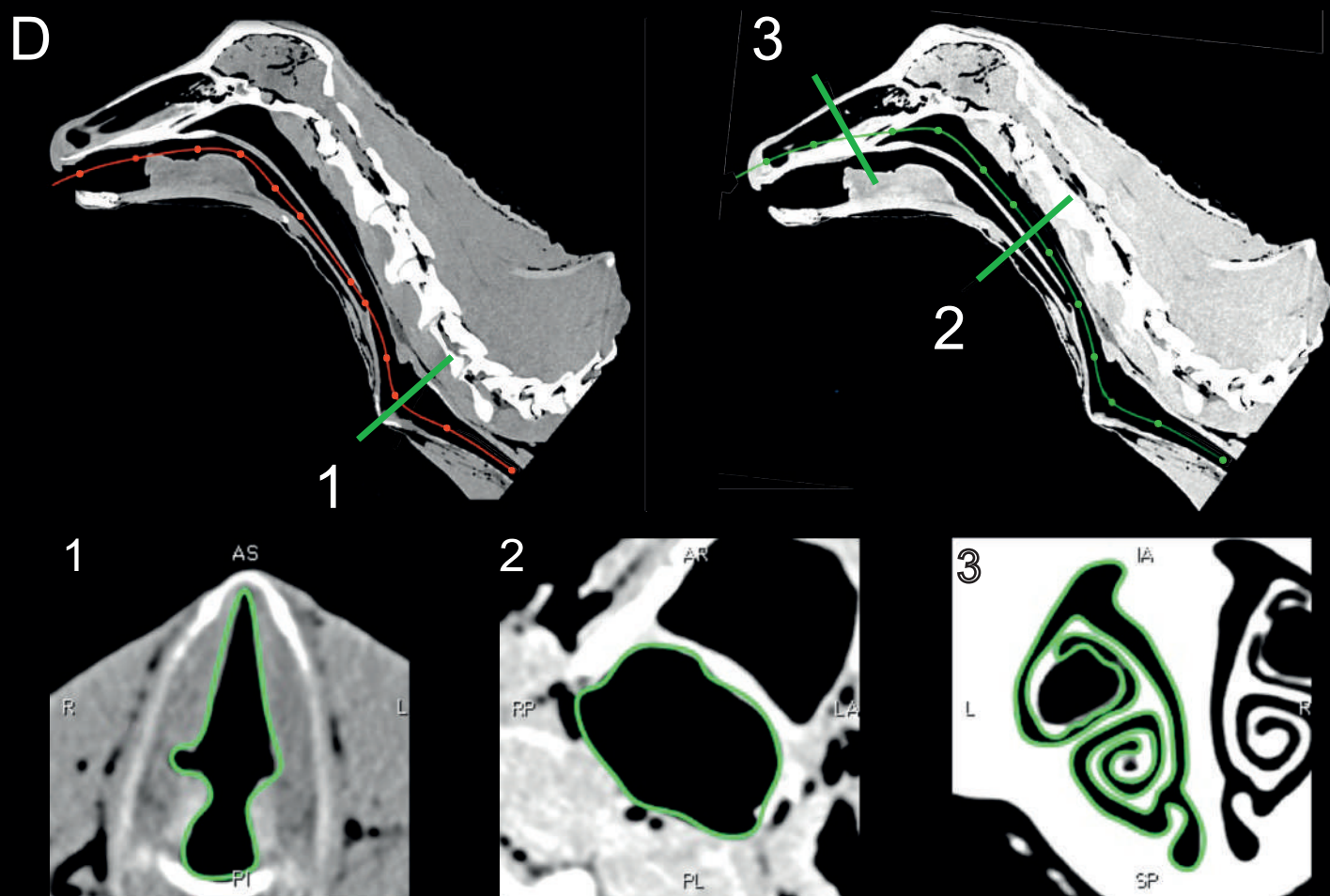
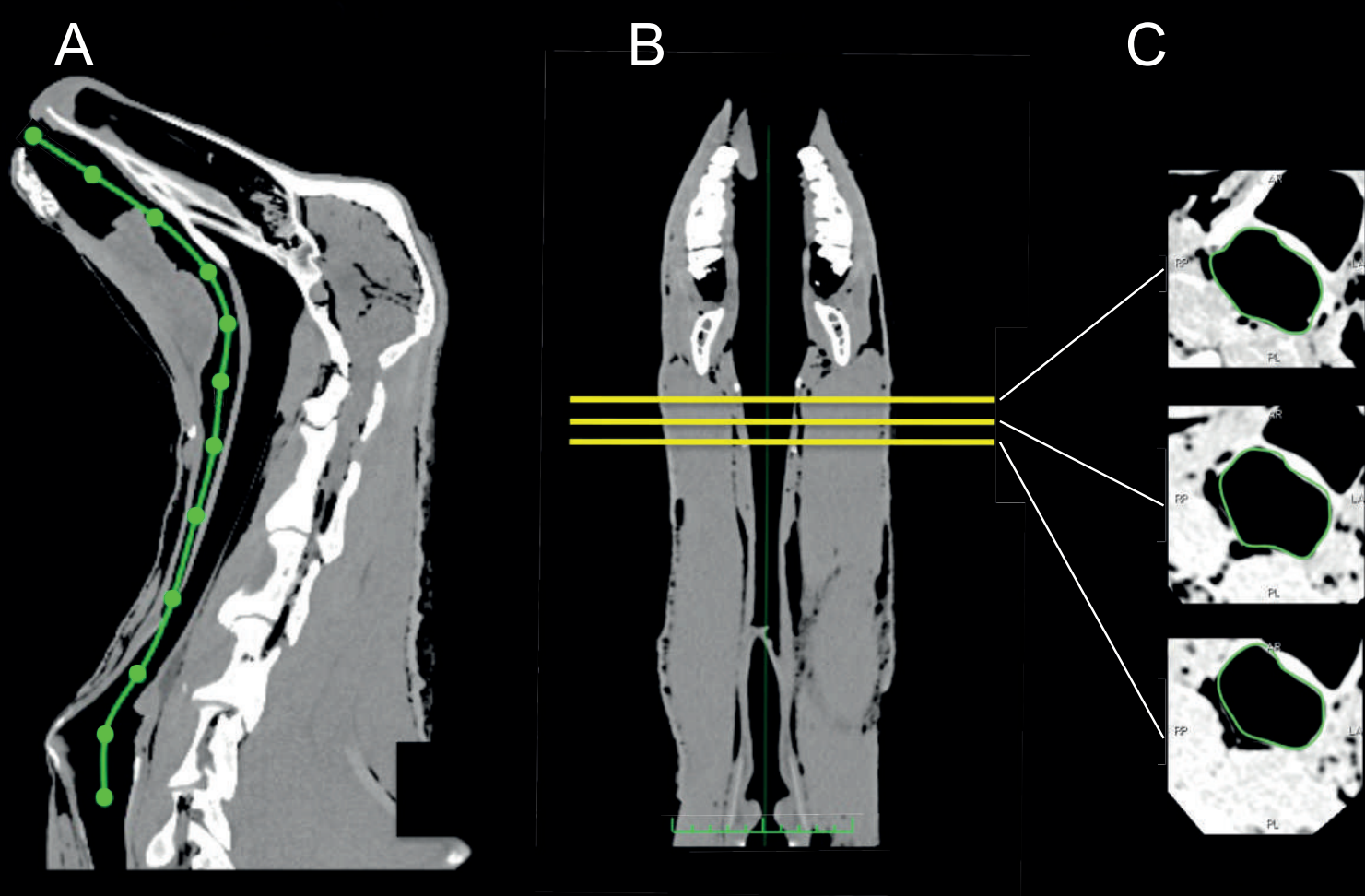


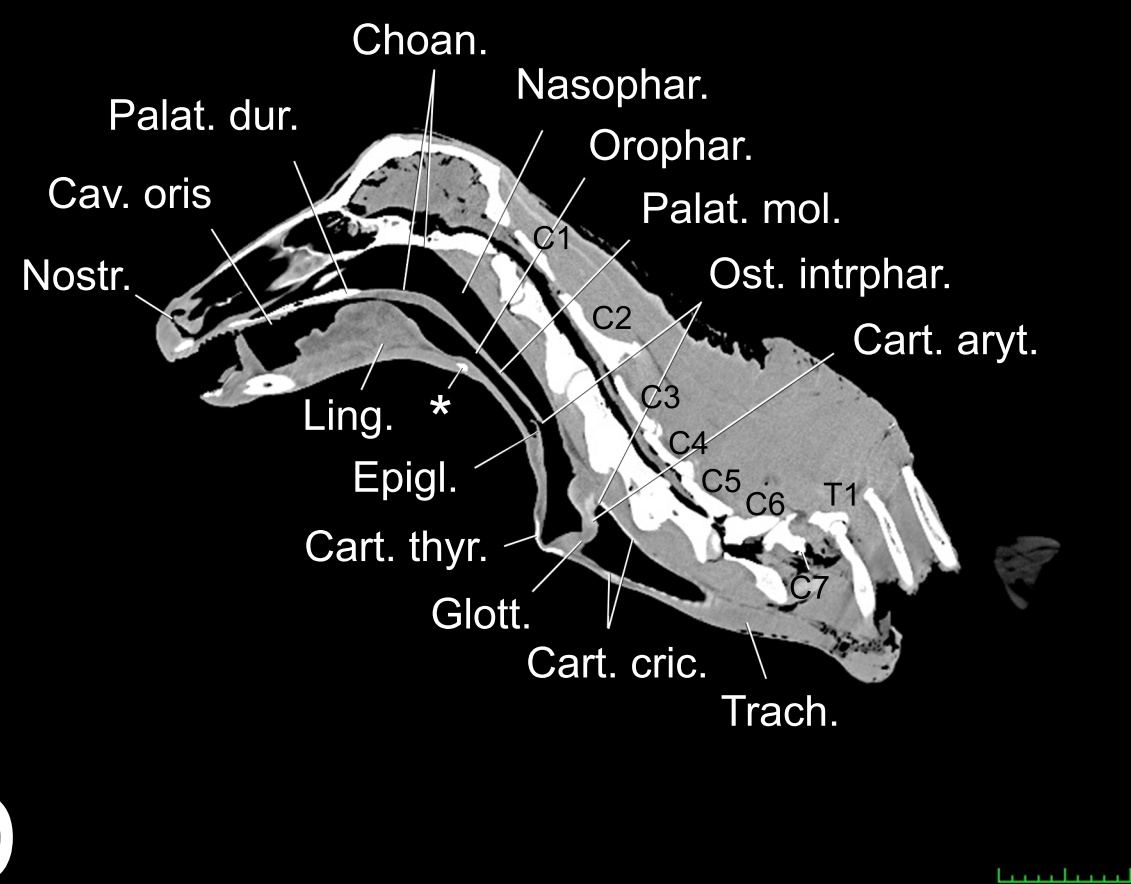
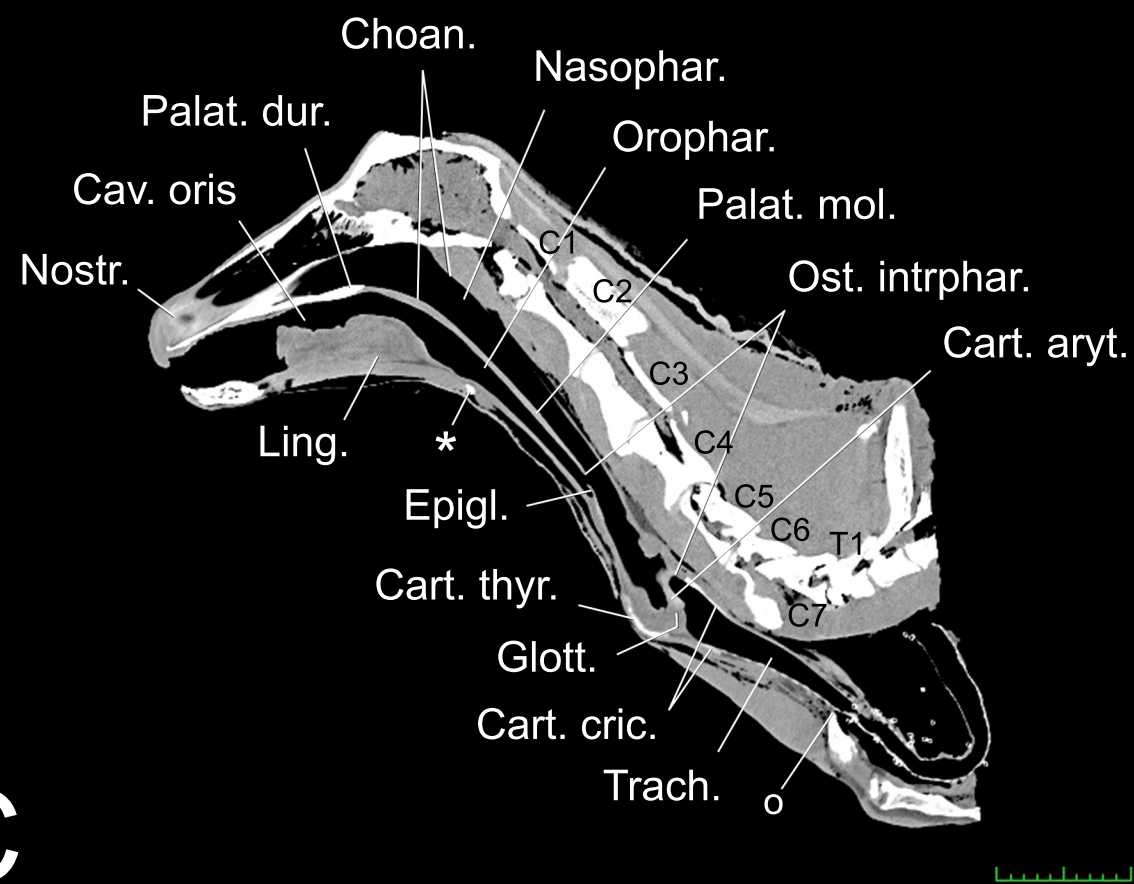
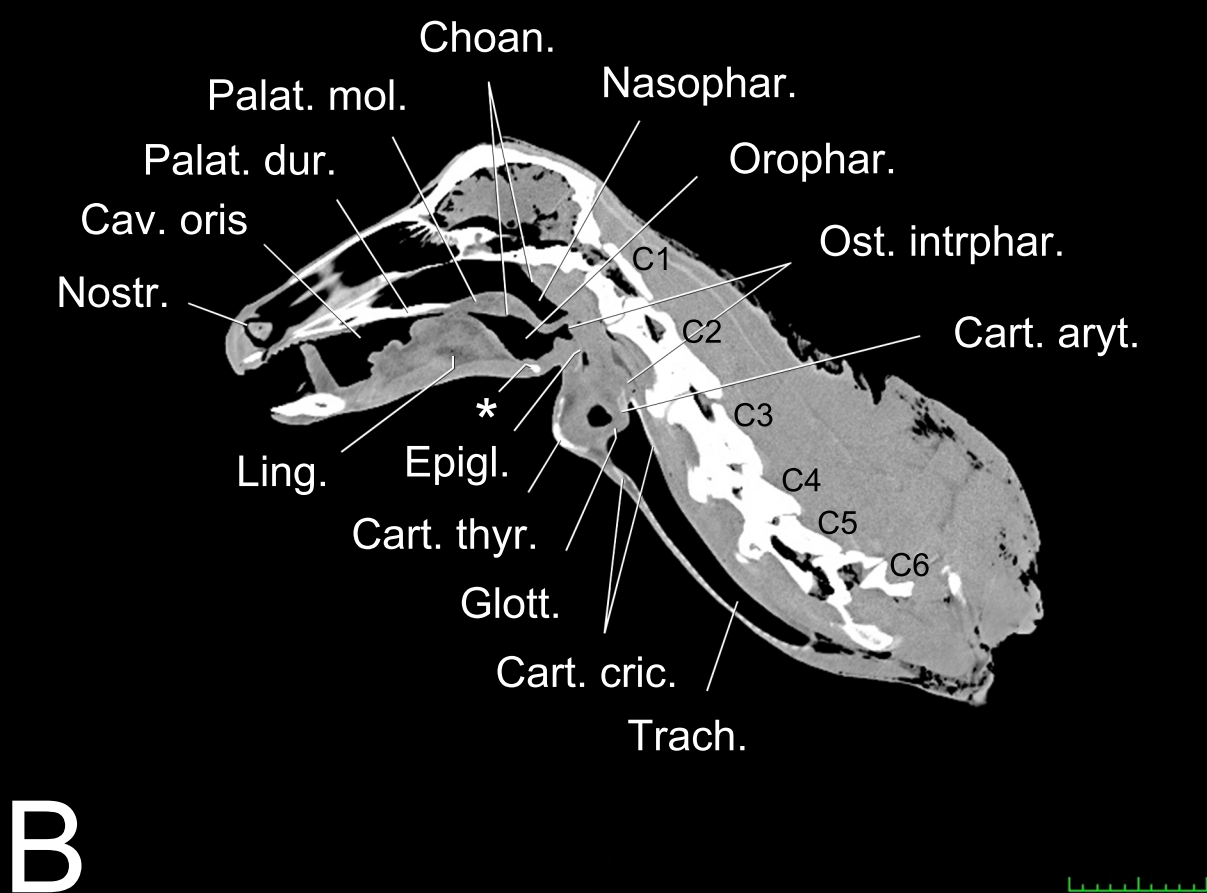
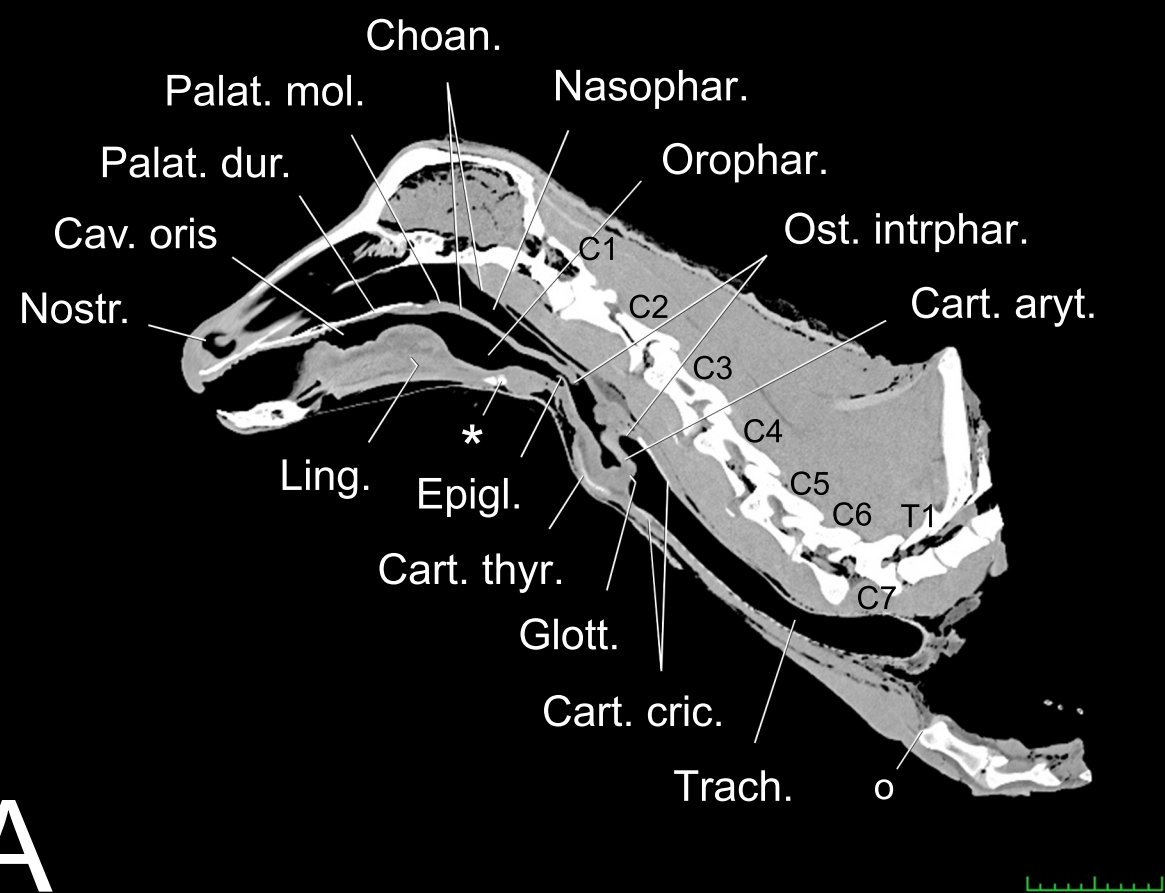


A

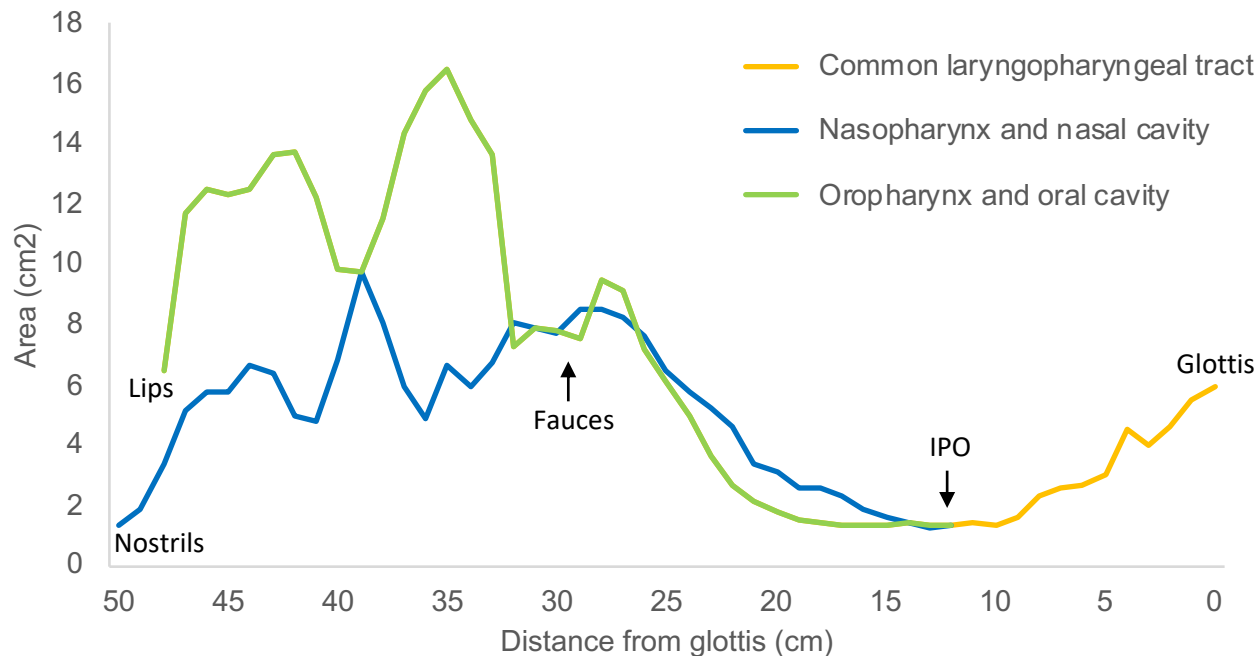


B





(A) Male 1



(B) Male 2

